Title:
CAD-based Adjoint Optimization using other Components in a CAD Model Assembly as Constraints

Authors:
Dheeraj Agarwal, dheeraj@liverpool.ac.uk, University of Liverpool
Trevor T. Robinson, t.robinson@qub.ac.uk, Queen's University Belfast
Cecil G. Armstrong, c.armstrong@qub.ac.uk, Queen's University Belfast

Keywords:
CAD, adjoint, optimization, assembly, constraints

DOI: 10.14733/cadconfP.2022.235-239

Introduction:
In general, mechanical design processes are not only driven by performance but are also subjected to constraints. These constraints may include the size of geometric features like the trailing edge radius of the turbine blade, volume or mass constraints, constraints on cross-sectional area, constraints on flow fields to account for a minimum lift, fixed exit-flow angle etc. Mader and Martins [7] used constraints such as bending moment, static and dynamic stability to examine optimal wing shapes in subsonic and transonic flows. Walther and Siva [11] presented an adjoint-based shape optimization for a multistage turbine design, with the objective to maximize the efficiency while constraining the mass flow rate and the total pressure ratio. Kontoleontos et al. [6] presented a constrained topology optimization approach for ducts with multiple outlets. The flow constraints are enforced at each outlet defining the volume flow rates, flow direction and/or mean temperature of the outgoing flow. In terms of geometrical constraints, Xu et al. [12] presented an approach employing a set of test points to impose the thickness and trailing edge radius constraint for the optimization of a nozzle guide vane.

When optimizing an industrial design, one of the important factors to consider is the packaging space in which the optimized component is expected to fit. This is typically constrained by other components in the assembly which define the regions the optimized shape is not allowed to violate. Since individual components are designed and optimized by different designers, when these are assembled together, issues such as fit often occur, requiring engineering changes late in the product development cycle [4]. Thus, it is important for designers and manufacturers to devise methods to ensure that the optimized component can be assembled within the space available before the actual component is manufactured. With the advances in CAD systems and development of the Digital Mock-Up (DMU) for complex CAD model assemblies, it is now possible to replace the physical prototypes with virtual ones and do the assembly of components in a virtual environment before any prototype is built. The DMU is a product assembly workbench where different components are positioned in 3D space relative to each other. Interference can occur during assembly when two or more components are designed such that they attempt to occupy the same physical space when assembled, and checks for this can be made in the DMU. An obvious step to stop clash appearing in the first place would be to include constraints imposed by adjacent components in the assembly during the design optimization of individual components, or to apply clash detection and fix the interferences during the product assembly.

Some of the early works in the field of interference detection between two solids are found in [2],[3]. Pan et al. [9] enabled interference detection directly using CAD models, while Zubairi et al. [13] developed a sensitivity approach to eliminate interference (if present) in a 3D CAD assembly, by identifying parameters defining the CAD features which need to be modified and calculating the

© 2022 CAD Solutions, LLC, http://www.cad-conference.net

amount of change required to eliminate interference. The approach is effective in eliminating interferences, but the effect of the resulted shape change on the performance of the individual components was not considered, meaning that the process of eliminating interference could reduce the performance of a product, or even make it unsuitable for its role. Recently, a 2D shape optimization of a NACA0012 aerofoil based on a polynomial response surface model was presented in [5], where assembly constraints were formulated to consider the presence of a fuel-box in the interior of the wing profile. The constraints were enforced as constant upper and lower bounds for the design parameters. Although the approach was successfully applied for optimization, using only the parameter bounds may be highly restrictive when the number of design variables increase.

In this paper, the research described has been used to optimize a component in terms of its performance, but with spatial constraints imposed within the CAD system. The developed approach is demonstrated on 2D and 3D parametric CAD models built in CATIA V5 and assembled with other components in CATIA V5 assembly workbench. Here, SU2 [8] is used for flow simulations, and Python 3.5 is used as the programming interface.

Interference Detection:

Interference occurs when some components in an assembly violate others by occupying the same physical space. The interference detection system in CATIA V5 provides capabilities to obtain the penetration depth between the interfering components. This is the minimum distance required to translate a product to avoid interference. In addition, the clearance distance between two components can be obtained.

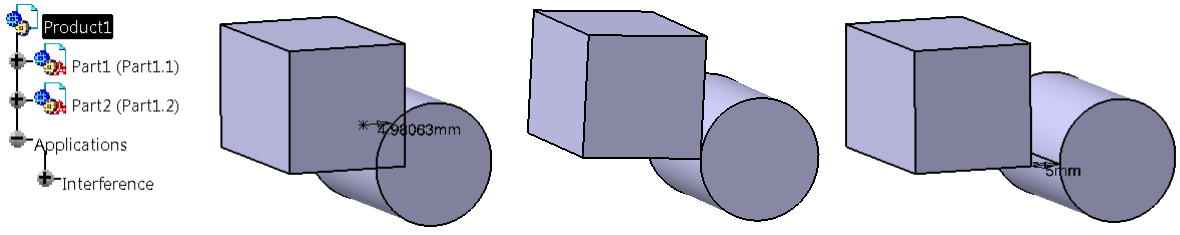

(a) (b) (c)

Fig. 1: Interference between two boxes as in CATIA (a) interference, (b) contact, and (c) clearance.

Fig. 1 displays the part-to-part interference detection in CATIA V5. It shows examples where the selected parts are in clash Fig. 1(a), are in contact Fig. 1(b), or have a clearance between them Fig. 1(c). A CAD system application programming interface (API) is developed in this work to automatically calculate the interference between the component being optimized and other assembly components. In this work, a positive value of interference defines the amount of penetration distance between the components, while the negative value defines the clearance distance.

From the perspective of optimization, the objective is to optimize a model such that the optimized shape has no interference with other components. It is therefore necessary to automatically compute the amount of interference between the CAD model being optimized and other components in the CAD model assembly. This is achieved by using a CAD system API which is configured to detect the components (other than the component being optimized) in the CATIA V5 product assembly module (i) and use the interference tool to compute the individual interferences with the initial CAD model ($\delta_i^{initial}$). At each optimization step, the CAD system API records the name of different components in the CAD product assembly and computes their interference values (used as assembly constraints). The other requirement is the computation of gradients of each assembly constraint with respect to the parameters used to define the initial CAD model. CATIA V5 offers capabilities to access the part model's parameterization through the assembly workbench. So, to compute the gradients of constraints, each parameter of the CAD model (j) is perturbed by a small amount ($\Delta\theta_j$), and the interference tool is used to obtain the new interference values (δ_i^j) for all components. In practice this

© 2022 CAD Solutions, LLC, http://www.cad-conference.net

is done at the same time as the design velocity computations. The respective gradients of the constraints are then obtained using a finite difference method as

$$gradient = \frac{\delta_i^j - \delta_i^{initial}}{\Delta\theta_j}. \quad (3)$$

Optimization Framework:

In this work, a gradient-based optimization technique is used to guide the design towards a local optimum over multiple optimization steps. Within each optimization step, the design variables are set to new values, causing a change in the objective function. A general optimization with assembly constraints can be defined as:

$$\begin{aligned} &\textit{Minimize:} && \textit{objective function,} \\ &\textit{Subject to:} && \delta_i^j < 0 \\ &\textit{design variables:} && \textit{vector of CAD parameter values} \end{aligned} \quad (4)$$

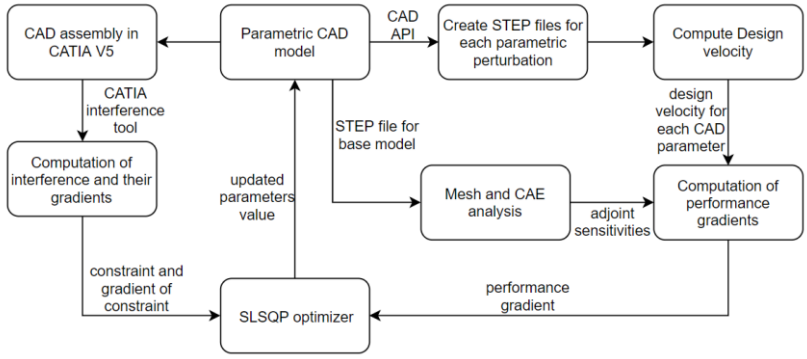

Fig. 2: CAD-based optimization using constraints from assembly components.

The optimization starts with a parametric CAD model, which is exported in a neutral CAD format i.e., STEP for creating the mesh and performing the CFD analysis. The resulting adjoint sensitivities are then used to calculate the gradient of the objective function with respect to CAD parameters using the approach described in [1]. The constraints due to interference with the adjacent components in the product assembly are enforced through an inequality constraint for the optimizer, such that the value of interference is less than zero. The flow diagram for the optimization process is shown in Fig. 2. The optimization framework is configured such that it uses the CAD system's API to automatically update the parameter values and subsequently use the updated part model in the assembly workbench to compute the interference from other components. Note, that while the STEP files are used in the computation of gradients, optimization is based on the native CAD file. In this work, the CAD models are created in CATIA V5 and optimized using sequential least square programming (SLSQP) method implemented in Scipy. SLSQP is a gradient-based optimization algorithm which minimizes a function with any combination of bounds, equality and inequality constraints.

Results:

The test case considered here is the benchmark two-dimensional NACA0012 aerofoil [10]. NACA0012 represents a symmetrical airfoil with zero chambers and 12% thickness to chord ratio. Here, the aerofoil is constructed using two Bézier curves, one defining the upper surface and one defining the lower surface. Each Bézier curve is defined by seven control points. The design variables are the Y-coordinates of the five-control point defining the upper and lower curves with the following constraints: the leading edge and trailing edge points are fixed, and the control points on each curve after the leading edge are constrained to move in equal and opposite directions, vertically offset from the leading-edge point. These constraints ensure C2 continuity at the leading edge. The initial profile of

© 2022 CAD Solutions, LLC, http://www.cad-conference.net

Bézier control points and resulting profile are shown in Fig. 3(a). Here, the airfoil is optimized (at zero angle of attack) using a total of five design variables resulting in a symmetrical flow around the airfoil. The flow conditions are defined as:

- Freestream Temperature = 273.15 K
- Freestream Mach number = 0.80
- Angle of attack (AOA) = 0 deg
- Objective Function = $min(C_d)$
- Design variables = 5

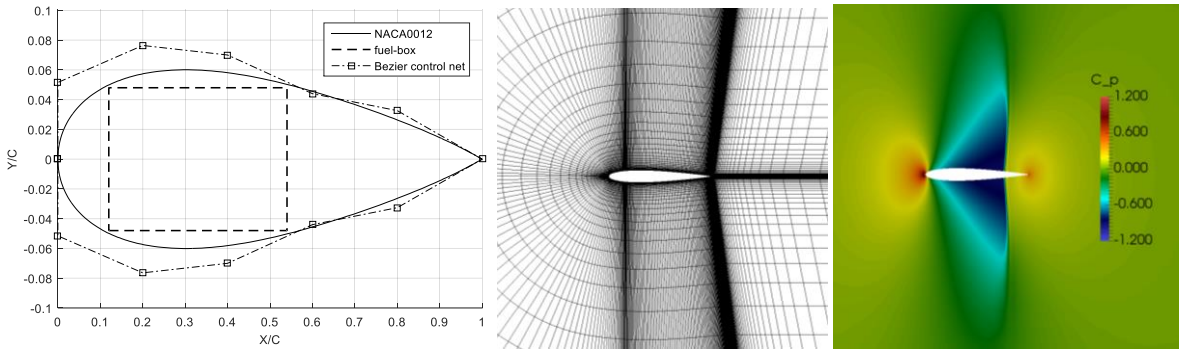

(a) (b) (c)

Fig. 3: **(a)** NACA0012 airfoil with Bézier control points and fuel-box, (b) Mesh around NACA0012 airfoil. (c) C_p distribution at the start of optimization.

The CFD mesh is created in ICEM-CFD using a multi-block strategy with 300 points on the airfoil and 51 points in the direction normal to the airfoil. A detailed view of the mesh around the aerofoil is shown in Fig. 3(b). The contour plot of the pressure coefficient (C_p) is shown in Fig. 3(c), where it can be seen that a strong shock-wave is formed at the upper surface of the airfoil, which contributes to increased drag on the airfoil. The automatic optimization framework described in section 4 is used to minimize the aerodynamic drag on the airfoil. The assembly constraint in this example is a rectangular fuel-box or battery profile around which the optimized airfoil must fit. Here, the 2D model was extruded by ± 1mm to create 3D geometry which was assembled with a solid model of the fuel-box in the CATIA V5 product assembly workbench. For each optimization step, a new CFD mesh is created in ICEM-CFD using an automated blocking script.

The optimization history of the aerofoil with the assembly constraint is shown in Fig. 4(a), where it is compared with the optimization when no such constraint exists. The drag coefficient is reduced from 0.04605 to 0.0091 when subjected to the assembly constraint compared to 0.00013 for an un-constrained optimization (with parameter bound). The optimized geometries are compared in Fig. 4(b), where the Y-axis is amplified to enhance visual comparison. The un-constrained optimization results in a thinner aerofoil, compared to that obtained in the presence of assembly constraints, but it clearly violates the space occupied by the fuel-box. The pressure distributions around the aerofoil is shown in Fig. 4(c). It should be noted that the ideal solution for the un-constrained optimization problem is a very thin airfoil but using the parameter bounds restricts the optimizer to result in such geometry.

Conclusions:

The constrained optimization employing the prior information from assembly components was successfully demonstrated for minimizing the objective function without violating the space available for storing other components in the assembly. Python CAD system APIs have been developed which interact with the product assembly module of CATIA V5 to extract interference distances between the component being optimized and other components to be assembled together.

© 2022 CAD Solutions, LLC, http://www.cad-conference.net

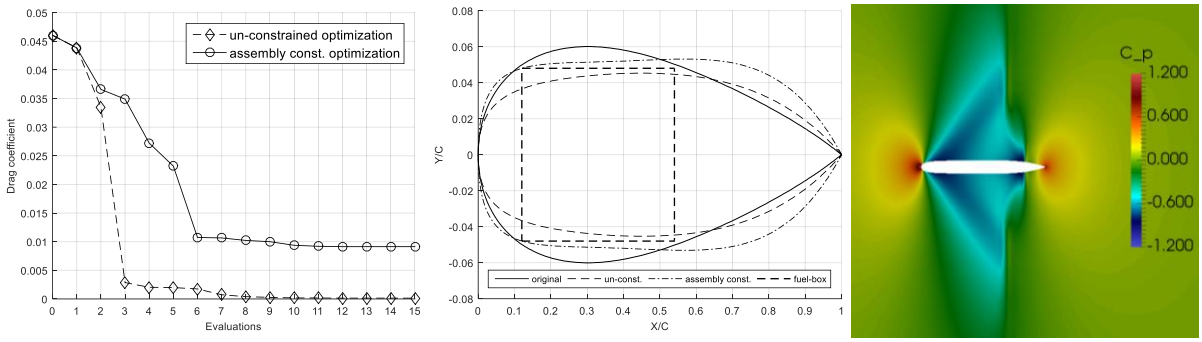

(a) (b) (c)

Fig. 4: NACA0012 optimization with and without assembly constraints. (a) function evaluations, (b) geometry comparison, (c) C_p contours on optimized NACA0012.

References:

[1] Agarwal, D.; Robinson, T.T.; Armstrong, C.G.; Marques, S.; Vasilopoulos, I.; Meyer, M.: Parametric design velocity computation for CAD-based design optimization using adjoint methods, Engineering with Computers, 34(2), 2018, 225-239, https://doi.org/10.1007/s00366-017-0534-x.

[2] Ahuja, N.; Chien, R.T.; Yen, R.; Bridwell, N.: Interference Detection and Collision Avoidance Among Three Dimensional Objects, AAAI-80 Proceedings, pp. 44-48.

[3] Boyse, J.W.: Interference detection among solids and surfaces, Communications of the ACM, 22(1), 1979, 3-9, https://doi.org/10.1145/359046.359048.

[4] Chang, K.-H.; Silva, J.; Bryant, I.: Concurrent design and manufacturing for mechanical systems, Concurrent Engineering, 7(4), 1999, 290-308, https://doi.org/10.1177/1063293X9900700403.

[5] Immonen, E.: 2D shape optimization under proximity constraints by CFD and response surface methodology, Applied Mathematical Modelling, 41(2017, 508-529, https://doi.org/10.1016/j.apm.2016.09.009.

[6] Kontoleontos, E.A.; Papoutsis-Kiachagias, E.M.; Zymaris, A.S.; Papadimitriou, D.I.; Giannakoglou, K.C.: Adjoint-based constrained topology optimization for viscous flows, including heat transfer, Eng. Optimization, 45(8), 2013, 941-961, https://doi.org/10.1080/0305215X.2012.717074.

[7] Mader, C.A.; Martins, J.R.R.A.: Stability-constrained aerodynamic shape optimization of flying wings, Journal of Aircraft, 50(5), 2013, 1431-1449, https://doi.org/10.2514/1.C031956.

[8] Palacios, F.; Alonso, J.J.; Duraisamy, K.; Colonno, M.; Hicken, J.; Aranake, A.; Campos, A.; Copeland, S.R.; Economon, T.D.; Lonkar, A.: 2013. Stanford University Unstructured (SU2): an open-source integrated computational environment for multi-physics simulation and design, 51st AIAA Aerospace Sciences Meeting including the New Horizons Forum and Aerospace Exposition. AIAA, Grapevine, Texas.

[9] Pan, C.; Smith, S.S.F.; Smith, G.C.: Determining interference between parts in CAD STEP files for automatic assembly planning, Journal of Computing and Information Science in Engineering, 5(1), 2005, 56-62, https://doi.org/10.1115/1.1861473.

[10] Vassberg, J.C.; Harrison, N.A.; Roman, D.L.; Jameson, A.: 2011. A systematic study on the impact of dimensionality for a two-dimensional aerodynamic optimization model problem, 29th AIAA Applied Aerodynamics Conference, Honolulu, HI.

[11] Walther, B.; Nadarajah, S.: Constrained adjoint-based aerodynamic shape optimization of a single-stage transonic compressor, Journal of turbomachinery, 135(2), 2013, 021017, https://doi.org/10.1115/1.4007502.

[12] Xu, S.; Jahn, W.; Müller, J.D.: CAD based shape optimization with CFD using a discrete adjoint, International Journal of Numerical methods in Fluids, 74(3), 2014, 153-168, https://doi.org/10.1002/fld.3844.

[13] Zubairi, M.S.; Robinson, T.T.; Armstrong, C.G.; Soban, D.S.: A sensitivity approach for eliminating clashes from computer aided design model assemblies, Journal of Computing and Information Science in Engineering, 14(3), 2014, 031002, https://doi.org/10.1115/1.4027345.

© 2022 CAD Solutions, LLC, http://www.cad-conference.net